Indian Journal of Experimental Biology
Vol. 64, June 2026, pp. 500-518
DOI: 10.56042/ijeb.v64i06.24625

Comparative bioactivities of native, degraded, and sulfated fucoidan derivatives from *Sargassum crassifolium*: insights from apoptosis, migration, immunostimulation, and multivariate analysis

Wei Cheng Hsiao[1†], Tien Chiu Wu[2†], Chen Che Hsieh[3], Pitchurajan Krishna Perumal[3], Yi Wen Chiu[4,5], Anil Kumar Patel[6,7,8]* and Chun Yung Huang[3]*

[1]Division of Gastroenterology (General medicine), Department of Internal Medicine, Yuan's General Hospital, Kaohsiung City 80249, Taiwan

[2]Department of Internal Medicine, Kaohsiung Medical University Hospital, Kaohsiung Medical University, Kaohsiung City 80756, Taiwan

[3]Department of Seafood Science, National Kaohsiung University of Science and Technology, Kaohsiung City 81157, Taiwan

[4]Division of Nephrology, Department of Internal Medicine, Kaohsiung Medical University Hospital, Kaohsiung Medical University, Kaohsiung City 80756, Taiwan

[5]Faculty of Medicine, College of Medicine, Kaohsiung Medical University, Kaohsiung City 80756, Taiwan

[6]Institute of Aquatic Science and Technology, National Kaohsiung University of Science and Technology, Kaohsiung City 81157, Taiwan

[7]Centre for Energy and Environmental Sustainability, Lucknow 226 029, Uttar Pradesh, India

[8]Department of Microbiology and Bioinformatics, Atal Bihari Vajpayee Vishwavidyalaya, Chhattisgarh, Bilaspur-495009, India

Received 11 November 2025; revised 17 January 2026

Native fucoidan (designated as SC) was extracted from *Sargassum crassifolium* following an extrusion-puffing pretreatment. SC was subjected to hydrogen peroxide (H_2O_2)-mediated degradation to yield a lower molecular weight derivative, SC-H_2O_2. Subsequently, two oversulfated derivatives were synthesized from SC-H_2O_2, namely SC-H_2O_2-S1 (mild sulfation), and SC-H_2O_2-S2 (intensive sulfation). All fucoidan derivatives induced apoptosis in A-549 cells via mitochondrial pathways, as evidenced by decreased MMP and Bcl-2 levels, increased Bax expression and cytochrome c release, and activation of caspases. Among them, SC-H_2O_2-S1 exhibited the strongest pro-apoptotic and anti-migration effects by modulating RANK and MMP-9 expressions. Additional experiments revealed that SC-H_2O_2 showed reduced immunostimulatory activity in RAW 264.7 murine macrophages compared to SC, whereas SC-H_2O_2-S1 enhanced the immunostimulatory effects relative to SC-H_2O_2. Principal component analysis (PCA) and hierarchical clustering analysis (HCA) indicated that SC and SC-H_2O_2 were characterized by modulation of apoptosis and immune-enhancing factors, whereas SC-H_2O_2-S1 and SC-H_2O_2-S2 exhibited stronger associations with apoptosis and cell migration.

Keywords: Cell migration, Fucoidan modification, Immunomodulatory activity, Mitochondrial apoptotic pathway

Introduction

Lung cancer, with its high incidence and significant morbidity and mortality rates, has led to extensive research endeavors aimed at enhancing its prevention, diagnosis, and treatment[1]. In recent years, lung cancer treatment has remained a considerable clinical challenge. Therefore, developing novel and natural agents and examining their therapeutic effects on lung cancer treatment is crucial.

Immunity constitutes the physiological capacity of organisms to identify and neutralize exogenous entities and pathogenic microorganisms through specialized defense mechanisms[2]. As the primary immunological barrier, innate immunity delivers rapid, nonspecific responses to infectious agents. Within this system, macrophages serve as essential effector cells, executing critical functions including immune surveillance, phagocytic clearance, chemotactic migration, and targeted pathogen destruction[3]. Following activation by diverse biological stimuli, macrophages acquire enhanced capacity to eradicate harmful substances and pathogens. A principal inflammatory mediator, nitric oxide (NO), is generated via inducible nitric oxide synthase (iNOS) in activated macrophages[4]. Macrophage activation commences when lipopolysaccharide

Correspondence:
E-mail: anilkpatel22@nkust.edu.tw
E-mail: cyhuang@nkust.edu.tw

(LPS), a structural component of Gram-negative bacterial membranes, engages the CD14/TLR coreceptor complex. This ligand-receptor interaction triggers phosphorylation cascades that ultimately induce iNOS expression[5], and concurrently stimulates release of cytokines and other inflammatory mediators. Consequently, macrophage activation pathways represent strategic targets for immune potentiation. Recent research has increasingly focused on natural polysaccharides due to their demonstrated capacity to modulate macrophage functions and strengthen innate immunity, highlighting their therapeutic potential as immunoenhancing agents[6].

Sargassum crassifolium is a brown macroalga (class Phaeophyceae) rich in bioactive polysaccharides, particularly fucoidan. Under favorable conditions, *Sargassum* species can proliferate rapidly, forming dense blooms that accumulate in coastal and port areas, where they disrupt ecosystems by reducing light penetration, altering water quality, and affecting oxygen availability. These events negatively impact fisheries, tourism, and coastal environments. Conversely, the abundant biomass represents a sustainable resource for fucoidan extraction with documented anticancer, antioxidant, and immunomodulatory activities. Therefore, effective utilization to reduce excessive *Sargassum* biomass is of both ecological and biotechnological importance[7]. Fucoidans are sulfated polysaccharides primarily composed of fucose, along with varying amounts of other monosaccharide residues, sulfate groups, and acetyl groups. These fucoidans have been shown to exhibit antioxidant, neuroprotective, antibacterial, anti-inflammatory, antitumor, as well as anticoagulant and antithrombotic biological effects[8]. Diverse biological effects of fucoidans are primarily determined by structural characteristics such as glycosidic branching patterns, sulfation levels and distribution, and molecular mass. Various strategies have been developed to obtain bioactive fucoidan derivatives. For example, Zhou *et al.*[9] reported the preparation and characterization of an acetylsalicylic-acid-modified fucoidan from *Undaria pinnatifida* (ASA-UPFUC), which exhibited enhanced antiproliferative activity against human non-small-cell lung cancer A549 cells. The derivative inhibited cell growth in a dose-dependent manner, achieving an IC_{50} of 49.09 μg mL^{-1}, and approximately 50 % lower than that of the unmodified *U. pinnatifida* fucoidan (UPFUC). In addition to such chemical modifications, the molecular weight and sulfate content of fucoidan derivatives represent other critical determinants of their biological activity. Low-molecular-weight (LMW) fucoidan is a sulfated polysaccharide derivative obtained from native fucoidan through various depolymerization processes. This fraction has attracted increasing scientific interest due to its diverse and potent biological activities, including anti-inflammatory, anticoagulant, anti-angiogenic, antithrombotic, antioxidant, and anti-obesity effects[10]. In addition, Hsiao *et al.*[11] found that derived fucoidans with differing sulfation levels and the oversulfation of fucoidan induces apoptosis in lung cancer cells, potentially through the Akt/mTOR/S6 signaling pathway. These effects were directly proportional to the degree of sulfation. Therefore, a notable correlation is suggested between the sulfate content of fucoidans and their biological characteristics. The present study investigates the biological activities of low-molecular-weight and oversulfated fucoidans, with a particular focus on their potential anti-lung-cancer effects.

Extrusion cooking is a high-temperature, short-time processing technology that combines intense shear, pressure, and thermal energy, and is widely applied in the food industry for cereal processing, protein texturization, shaping, and expansion[12]. During extrusion, multiple physicochemical transformations occur simultaneously, including mixing, grinding, starch gelatinization, protein denaturation, structural expansion, and inactivation of microorganisms and undesirable compounds. Compared with conventional thermal treatments, extrusion offers high throughput, precise process control, energy efficiency, and improved retention of nutritional quality[13]. When employed as a pretreatment strategy, extrusion induces profound structural and physicochemical modifications in raw materials. The combined effects of shear and heat disrupt cell walls, reduce matrix compactness, and increase surface area, thereby enhancing mass transfer and accessibility of intracellular constituents. These changes facilitate subsequent extraction or bioconversion processes, improve nutrient bioavailability and digestibility, and reduce antinutritional factors. Moreover, extrusion pretreatment is rapid, scalable, and cost-effective, with adjustable parameters such as moisture content, screw speed, and temperature enabling tailored modification of diverse biomass feedstocks[14]. Consequently, extrusion pretreatment has been reported to enhance the release of functional components, including soluble dietary fibers and phenolic compounds, although its application for

improving polysaccharide extraction efficiency remains relatively underexplored.

In this study, a degraded fucoidan (SC-H_2O_2) was generated by hydrogen-peroxide treatment of pre-extracted SC. Two oversulfated derivatives were subsequently synthesized: SC-H_2O_2-S1, produced by mild oversulfation with SO_3-DMF, and SC-H_2O_2-S2, obtained by intensive oversulfation under the same reagent system. These preparations were evaluated for their anti-proliferative activity and capacity to modulate cell migration in human lung carcinoma A549 cells, as well as for their immunomodulatory effects in RAW 264.7 macrophages. To address analytical complexity and clarify relationships among variables and samples, principal component analysis (PCA) and hierarchical clustering analysis (HCA) were applied. To the best of the authors' knowledge, this study is the first to elucidate potential anti-lung cancer and immunomodulatory mechanisms of combined low-molecular-weight (LMW) and oversulfated fucoidan derivatives derived from single-screw extrusion-pretreated *Sargassum crassifolium*. The results demonstrate that this combination effectively suppresses human lung cancer cell proliferation while enhancing immunostimulatory activity, highlighting its potential as a chemopreventive adjuvant for lung cancer and immunodeficiency-related disorders. Overall, the findings confirm that precise modulation of fucoidan molecular weight and sulfation degree critically governs its biological activities.

Materials and Methods

Materials

Brown seaweed biomass (*S. crassifolium*) was collected from Kenting (Pingtung, Taiwan). Chemical reagents were obtained as follows: molecular weight standards (dextrans: 5, 50, 150, 670 kDa), monosaccharides (D-glucuronic acid, D-galacturonic acid, L-fucose, D-galactose, D-mannose, D-xylose), and specialty chemicals, including 2,2,2-trifluoroacetic acid, dimethyl sulfoxide, potassium bromide, and 3-(4,5-dimethylthiazol-2-yl)-2,5-diphenyltetrazolium bromide (MTT) were acquired from Sigma-Aldrich (St. Louis, MO, USA). Cell culture reagents, including Dulbecco's Modified Eagle Medium (DMEM), Ham's F12K medium, fetal bovine serum (FBS), penicillin streptomycin solution, and trypsin/EDTA, were obtained from Gibco Laboratories in Grand Island, New York, USA. Fluorescent probes, namely tetramethylrhodamine ethyl ester (TMRE) and fluorescein isothiocyanate (FITC)-conjugated anti-Bcl-2 antibodies, were purchased from Molecular Probes, Invitrogen, Carlsbad, California, USA. Alexa Fluor® 488-tagged anti-iNOS and phycoerythrin (PE)-labeled anti-COX-2 antibodies were supplied by Cell Signaling Technology, Beverly, Massachusetts, USA. All other biochemicals and immunological reagents were sourced from Sigma Aldrich.

Extrusion method

The extrusion processing employed followed a previous method[15]. Extrusion pretreatment was carried out using a laboratory-scale single-screw extruder (Tsung Hsing Co. Ltd., Kaohsiung, Taiwan) equipped with a 74 mm screw (length-to-diameter ratio of 3.07) and a 5 mm rounded die. *S. crassifolium* biomass was adjusted to 35% moisture prior to processing. The extruder was operated at a feed rate of 10.4 kg h^{-1}, a barrel temperature of 115 °C, and a screw speed of 360 rpm. These parameters, optimized in our previous work[15], enabled stable and reproducible steady-state extrusion. Post-extrusion, products were immediately dried (55°C, 30 min), ambient-cooled, and then ground. Final particulates were packaged in aluminum barrier pouches under refrigerated storage (4°C) pending subsequent extraction procedures.

Polysaccharide extraction method

Native fucoidan was obtained from extrusion-pretreated *S. crassifolium* via a method detailed previously[16]. The extracted material was stored in aluminum barrier pouches at 4°C until required for subsequent experiments. The yield of the extraction process was calculated according to Equation (1):

$$Yield\ (\%) = (W_{ES}/W_S) \times 100 \quad \ldots (1)$$

Where W_{ES} – weight of extracted solids, and W_S – weight of sample

Preparation of degraded fucoidan

Primary degradation of native fucoidan was performed using hydrogen peroxide (H_2O_2), following a method described in the literature[15]. Briefly, 200 mg of native fucoidan was dissolved in 20 mL of double distilled water, followed by the addition of hydrogen peroxide to a final concentration of 20 mM to initiate depolymerization. The reaction was carried out with continuous stirring at 25 °C for 16 h. Upon completion, the degraded polysaccharide was precipitated by adding aqueous ethanol to a final concentration of 75 percent. The precipitate was collected

by centrifugation at 9,170 *g* for 30 min and subsequently freeze dried.

Sulfation of fucoidan

Sulfation of SC-H_2O_2 was performed according to the previously described method[11]. The sulfating reagent, sulfur trioxide dimethylformamide complex (SO_3-DMF), was prepared by slowly adding 20 mL of chlorosulfonic acid to 100 mL of N,N dimethylformamide under cooling in an ice water bath. Dried SC-H_2O_2 (0.1 g) was dispersed in 10 mL of formamide (FA) and stirred at room temperature for 30 min to ensure complete solubilization. Subsequently, 10 mL of the sulfation reagent was added to obtain SC-H_2O_2-S1, whereas 20 mL was used to produce SC-H_2O_2-S2. The reaction was allowed to proceed for 4 h, after which the solution was neutralized to pH 7.0 and dialyzed against distilled water using a membrane with a molecular weight cutoff of 1 kDa. The dialysate was then concentrated and freeze dried to yield the oversulfated fucoidan derivatives.

Analytical methods

The total sugar content was quantified using the phenol-sulfuric acid method, employing L-fucose as the standard reference. Based on this standard, fucose levels were subsequently estimated following the procedure described by Yang *et al.*[17]. The determination of sulfate content was carried out using a previously reported method[11]. Briefly, the samples were subjected to acid hydrolysis at 105 °C for 5 h in 1 N hydrochloric acid. The resulting sulfate content was quantified by ion chromatography using a Dionex ICS-1500 system (Dionex Corporation, Sunnyvale, CA, USA) fitted with an IonPac AS9-HC column. Separation was carried out at a flow rate of 1 mL/min with 9 mM sodium carbonate as the mobile phase. Potassium sulfate was used to generate the calibration curve, and sulfate ions were detected by conductometric detection.

Monosaccharide composition using HPLC

Monosaccharide compositional analysis was conducted following a previous method[11]. Monosaccharide composition was determined following acid hydrolysis with 2 M trifluoroacetic acid (TFA) at 110 °C for 4 h. After removal of residual TFA, both polysaccharide samples and monosaccharide standards were derivatized with 1-phenyl-3-methyl-5-pyrazolone (PMP) at 70 °C for 100 min. The resulting reaction mixtures were subjected to three successive chloroform extractions to obtain purified PMP derivatives. Chromatographic analysis was performed on a Shimadzu high-performance liquid chromatography system equipped with an Inspire™ C18 column (250 × 4.6 mm, 5 μm) maintained at 25 °C. Elution was carried out isocratically at a flow rate of 1 mL/min using a mobile phase consisting of 0.1 M phosphate buffer (pH 6.7) and acetonitrile in an 83:17 volume ratio. Detection was conducted by UV visible absorbance at 245 nm with an injection volume of 20 μL. The monosaccharide standards were D-glucuronic acid, D-galacturonic acid, L-fucose, D-galactose, D-mannose, and D-xylose.

Molecular weight determination

A Shimadzu high-performance liquid chromatography (HPLC) system (Shimadzu, Kyoto, Japan) was utilized for polysaccharide molecular weight analysis following a previous method[15]. Dextrans with varying molecular weights (5, 50, 150, and 670 kDa) were used as the MW standards.

Fourier transform infrared (FTIR) spectroscopy

FTIR spectra were obtained using a previous procedure described by Hsiao *et al.*[15]. In brief, the sample was thoroughly mixed with potassium bromide (KBr) at a mass ratio of 1:50 and finely ground until the particle size was reduced to less than 2.5 μm. The resulting mixture was compressed under vacuum at 500 kg/cm² to produce transparent KBr pellets. Fourier transform infrared spectra were recorded using an FT 730 spectrometer manufactured by Horiba in Kyoto, Japan. Data acquisition was performed over 60 accumulated scans at a resolution of 16 cm^{-1} across the spectral range from 4000 to 400 cm^{-1}.

Nuclear magnetic resonance (NMR) spectroscopy

The NMR spectra were acquired using a method previously reported by Hsiao *et al.*[15]. Fucoidan samples were dissolved in 99.9 percent deuterium oxide (D_2O) directly in NMR tubes prior to analysis. Nuclear magnetic resonance spectra were recorded using a Varian VNMRS 700 spectrometer manufactured by Varian Inc. in Palo Alto, California, USA, to characterize the structural features of the polysaccharides.

Cell culture

The Bioresource Collection and Research Center (BCRC), located in Hsinchu City, Taiwan, provided human lung cancer A-549 (BCRC number 60074) and

murine macrophage cell lines RAW 264.7 (BCRC No. 60001) for procurement. The culture medium used for A-549 cells was Ham's F12K medium, and for RAW 264.7 cells was DMEM medium. The plain medium was combined with 10% FBS, 100 μg/mL streptomycin, and 100 units/mL penicillin to create the complete medium. Every two to three days, the cells in each culture were subcultured, and all conditions were kept at 37°C with humidified 5% CO_2.

Cell viability analysis

Cell viability was assessed through the MTT assay as described previously[15]. The percentage of viable cells was determined using the equation (2):

$$Cell\ viability\ (\%) = (A_T/A_C) \times 100 \quad \ldots (2)$$

A_T was the absorbance at 570 nm in the test, and A_C was the absorbance at 570 nm for the control.

Flow cytometry-based analyses

The A-549 cells with a cell density 4×10^4 cells/mL were cultured without (cells were in serum-free medium, as a control) and with 200 μg/mL SC, SC-H_2O_2, SC-H_2O_2-S1, and SC-H_2O_2-S2 (cells were in serum-free medium) for 48 h, and then cells were collected for flow cytometer-based analysis as the described protocols: (1) For the MMP analysis, the cells were labeled with TMRE (100 nM). (2) For the Bcl-2 expression analysis, the cells were labeled with FITC-anti-Bcl-2 antibody (1:25, v/v). (3) For the Bax expression analysis, the cells were labeled with FITC-anti-Bax antibody (1:25, v/v). (4) A 1:10 (v/v) FITC-anti-cytochrome c antibody was applied to label the cell preparations for the cytochrome c release experiment. (5) The cells were labeled with FITC-LEHD-FMK for caspase-9 detection, FITC-IETD-FMK for caspase-8 detection, and FITC-DEVD-FMK for caspase-3 detection. (6) The cells were double-stained with annexin V-FITC (1:20, v/v) and PI (1:20, v/v) for the annexin V-FITC / PI staining experiment. (7) The cells were stained with PE-anti-RANK antibody (1:20, v/v) and Alexa Fluor 488-anti-MMP-9 antibody (1:20, v/v) for the receptor activators of nuclear factor kappa-B (RANK) and matrix metalloproteinase-9 (MMP-9) expression analyses, respectively. Quantification of fluorescent cells was performed using a previously reported method[18].

Transwell cell migration analysis

A-549 cells were seeded at a density of 1×10^5 cells per well into the upper chamber of a transwell system, containing 500 μL of serum-free medium, either untreated or supplemented with SC, SC-H_2O_2, SC-H_2O_2-S1, or SC-H_2O_2-S2 at a concentration of 200 μg/mL. The lower chamber was filled with 1 mL of complete culture medium as a chemoattractant. After a 48-hour incubation at 37°C in a 5% CO_2 atmosphere, non-migrated cells on the upper membrane surface were gently scraped off. Migrated cells on the lower membrane were stained with 0.1% crystal violet and observed under a microscope. The stained cells were then solubilized with alcohol, and absorbance at 590 nm was measured using an ELISA plate reader to quantify migration.

Measurement of Nitrite Oxide in Culture Media

RAW 264.7 cells were plated at a density of 2×10^5 cells/mL in 96-well flat-bottom plates and cultured for 24 hours at 37 °C in a humidified atmosphere containing 5% CO_2. After this initial incubation, the medium was aspirated and replaced with fresh medium supplemented with either 1 μg/mL LPS or 500 μg/mL of SC, SC-H_2O_2, SC-H_2O_2-S1, or SC-H_2O_2-S2. The following procedures were conducted as a previously published method[15].

Quantitation of Cytokines by ELISA

RAW 264.7 cells were incubated at 37 °C in a humidified 5% CO_2 environment for 24 hours. Following this incubation, the existing medium was discarded and replaced with fresh medium containing 1 μg/mL LPS (positive control) and 500 μg/mL of SC, SC-H_2O_2, SC-H_2O_2-S1, or SC-H_2O_2-S2. After an additional 24-hour treatment period, the liquid media were collected, and the levels of TNF-α, IL-6, and IL-1β were measured spectrophotometrically using ELISA Max kits (BioLegend, San Diego, CA, USA) following the protocol provided by the supplier.

Measurement of iNOS and COX-2 expressions

RAW 264.7 cells at a density of 4×10^5 cells/mL were cultured either without treatment (as a non-treated control) or with 1 μg/mL LPS or 500 μg/mL of SC, SC-H_2O_2, SC-H_2O_2-S1, or SC-H_2O_2-S2 for 24 hours. After treatment, the cells were collected for flow cytometry analysis. The cells were stained with iNOS-Alexa® 488 antibody (1:50, v/v) or COX-2-PE antibody (1:50, v/v). Quantification of fluorescent cells was performed using a previously reported method[18].

Statistical analysis

All experiments were conducted in triplicate, and the results were presented as mean ± standard

deviation. Statistical comparisons were carried out using one-way ANOVA, followed by Duncan's multiple range test to assess differences between groups. A p-value less than 0.05 was considered statistically significant. PCA was conducted to explore the associations between measured parameters and sample groups (SC, SC-H_2O_2, SC-H_2O_2-S1, and SC-H_2O_2-S2). HCA was additionally performed to classify the samples based on these variables. All multivariate analyses were executed using R software (version 4.4.3).

Results and Discussion

Preparation of degraded and oversulfated fucoidans from extrusion-pretreated *S. crassifolium*

A comprehensive presentation of the preparation processes for SC, SC-H_2O_2, SC-H_2O_2-S1, and SC-H_2O_2-S2 is presented in Supplementary Fig. S1. In the present study, the collected *S. crassifolium* biomass was pretreated using an extrusion-puffing method before the extraction of fucoidan. Next, native fucoidan (SC) was acquired. The fucoidan extraction yields from extrusion-pretreated and non-extruded *S. crassifolium* were 11.3 ± 1.3 g/100g and 2.69 ± 0.97 g/100g, respectively. These results demonstrate that the extrusion process significantly enhances the fucoidan extraction yield, increasing it by approximately 4.2-fold (11.3/2.69 = 4.2). The results were superior to our previous report[15], possibly due to different *Sargassum* species. In this study, oxidative degradation was employed to depolymerize polysaccharides. This approach offers several advantages over conventional degradation methods. First, it can be conducted in aqueous media under moderate temperatures without the use of strong acids or bases, which simplifies operation and minimizes post-reaction cleanup compared to harsh hydrolytic processes. Second, oxidative depolymerization can enhance or modulate the bioactivity and functional properties of polysaccharides. For instance, partial degradation often improves bioavailability, antioxidant capacity, or other biological activities, while enabling the generation of functional oligomers or polymer derivatives with potential applications in biomedical and food industries. Third, oxidative methods generally produce fewer toxic by-products and allow for simpler downstream processing. In particular, oxidative routes utilizing hydrogen peroxide or catalytic systems are considered more environmentally friendly than acid- or alkali-based hydrolysis, as they reduce neutralization waste and align with greener chemistry principles[19,20]. SC was subsequently subjected to oxidative degradation with hydrogen peroxide (H_2O_2), affording a degraded fucoidan derivative referred to as SC-H_2O_2. Although fucoidan is intrinsically a sulfated polysaccharide, additional sulfonation is frequently employed to further modulate its biological performance. The degree and distribution of sulfate groups critically influence fucoidan's physicochemical properties, charge density, and interactions with biomolecules. Increased sulfation enhances electrostatic interactions with positively charged proteins, enzymes, and cell surface receptors, thereby improving activities related to inflammation, coagulation, and viral inhibition. Numerous studies have demonstrated that sulfate content is a principal determinant of fucoidan's antioxidant, anticoagulant, antiviral, and anti-inflammatory functions[21]. Moreover, experimental enrichment of sulfate groups, such as in fucoidan derived from *Sargassum siliquosum*, has been shown to significantly elevate antioxidant efficacy compared with native counterparts[22]. Sulfate moieties also provide reactive sites for secondary functionalization, including metal ion complexation, which can further enhance antimicrobial and antiviral properties. Collectively, controlled sulfonation represents an effective strategy to tailor fucoidan for advanced biomedical and functional applications[23]. Subsequently, SC-H_2O_2 was used as the starting material for the preparation of oversulfated fucoidan derivatives. Mild sulfonation using the SO_3-DMF yielded SC-H_2O_2-S1, whereas more intensive sulfonation under the same reagent system produced SC-H_2O_2-S2. The resulting derivatives were comprehensively characterized using physicochemical, compositional, and structural analytical approaches.

Physicochemical and compositional analyses of SC, SC-H_2O_2, SC-H_2O_2-S1, and SC-H_2O_2-S2

As shown in Table 1, the peak molecular weight (MW) and distribution range of SC were 328.5 kDa and 193.4-836.0 kDa, respectively. Following oxidative degradation, SC-H_2O_2 exhibited a markedly reduced peak Mw of 122.8 kDa with a narrower distribution range of 37.6-275.8 kDa. Similarly, both SC-H_2O_2-S1 and SC-H_2O_2-S2 displayed the same peak Mw of 122.8 kDa; however, their Mw distributions were more restricted (61.9-167.6 kDa). The narrower Mw distribution observed in SC-H_2O_2-

S1 and SC-H_2O_2-S2 after oversulfation indicated that this modification benefits further enhancing the uniformity of the fucoidan molecular size distribution. A comparison of SC (328.5 kDa) and SC-H_2O_2 (122.8 kDa) revealed a decrease of approximately 62.6% (100 – ((122.8/328.5)×100)) in peak Mw, demonstrating the effectiveness of oxidative degradation in reducing polysaccharide molecular size. The number-average molecular weight (Mn), weight-average molecular weight (Mw), and polydispersity index (PDI) values for SC, SC-H_2O_2, SC-H_2O_2-S1, and SC-H_2O_2-S2 are presented in Table 1. Among these derivatives, SC-H_2O_2-S1 exhibited the lowest PDI, indicating the narrowest and most uniform molecular weight distribution. However, the differences in PDI between SC-H_2O_2-S1 and the other derivatives were not substantial. Table 1 summarizes the chemical compositions of SC, SC-H_2O_2, SC-H_2O_2-S1, and SC-H_2O_2-S2. Overall, the trends in total sugar and fucose contents were similar, both showing a decrease after degradation. This reduction can be attributed to the cleavage of glycosidic bonds and oxidative modification of monosaccharide units during chemical or oxidative treatments (e.g., H_2O_2 process), which can lead to the loss of fucose and other monosaccharide residues. Consequently, a smaller proportion of intact carbohydrate remains within the polymeric fraction, thereby lowering the measured total sugar content[24]. In addition, degradation often generates oligosaccharides and soluble fragments that may be lost during purification, further reducing the recovered carbohydrate content[25]. In contrast, moderate oversulfation may lead to an apparent increase in total sugar content, which can be attributed to improved solubility and dispersibility of the polysaccharides. These properties facilitate more efficient carbohydrate recovery in aqueous assay systems and reduce losses caused by aggregation or precipitation[21]. However, when sulfation is conducted under excessively severe conditions, cleavage of glycosidic linkages or chemical modification of sugar residues may occur, resulting in partial desugaring. The resulting low molecular weight fragments are prone to removal during dialysis or precipitation steps or may exhibit reduced reactivity in conventional sugar assays, thereby decreasing the measured sugar content[11]. Moreover, compared with the degraded precursor, both sulfated derivatives show changes in fucose content, which reflect structural remodeling during the sulfonation process. These changes arise because the introduction of sulfate groups can occur at specific hydroxyl positions on sugar residues, including fucose, and may preferentially modify or substitute fucose units. In addition, harsher sulfation conditions that generate SC-H_2O_2-S2 may lead to partial cleavage of labile glycosidic bonds and loss of fucose-rich oligomers during purification, thereby reducing the relative fucose content[26]. Consistent with this interpretation, previous studies on oversulfated

Table 1 — Molecular weight and chemical composition analyses of SC, SC-H_2O_2, SC-H_2O_2-S1, and SC-H_2O_2-S2.

Molecular weight (MW)	SC	SC-H_2O_2	SC-H_2O_2-S1	SC-H_2O_2-S2
Peak MW [1] (kDa)	328.5	122.8	122.8	122.8
MW range (kDa)	193.4-836.0	37.6-275.8	61.9-167.6	61.9-167.6
Mn (number-average MW, kDa)	387.7	120.1	121.6	112.7
Mw (weight-average MW, kDa)	442.1	139.7	128.0	125.9
PDI (polydispersity index)	1.09	1.16	1.05	1.12
Chemical composition	SC [3]	SC-H_2O_2 [3]	SC-H_2O_2-S1 [3]	SC-H_2O_2-S2 [3]
Total sugar (%) [2]	45.6 ± 0.8 [c]	30.8 ± 0.2 [a]	46.8 ± 0.4 [d]	33.3 ± 0.2 [b]
Fucose (%) [2]	27.3 ± 1.6 [b]	20.1 ± 1.7 [a]	24.5 ± 1.2 [b]	19.1 ± 2.1 [a]
Sulfate (%) [2]	18.6 ± 1.4 [a]	19.2 ± 0.8 [a]	40.1 ± 3.7 [b]	55.2 ± 2.4 [c]
Monosaccharide composition (molar ratio)	SC	SC-H_2O_2	SC-H_2O_2-S1	SC-H_2O_2-S2
Fucose	1	1	1	1
Galactose	0.24	0.27	0.26	0.30
Glucuronic acid	0.19	0.07	N.D. [4]	N.D.
Galacturonic acid	0.15	0.06	N.D.	N.D.
Mannose	0.08	0.07	0.07	0.08
Xylose	0.04	0.10	N.D.	0.08

[1] Peak Mw: molecular weight of the highest peak. [2] The percentages of total sugars, fucose, and sulfate are calculated as (g/g, dry basis) × 100. [3] Triplicate experiments were conducted; values in the same row with different letters ([a], [b], [c], [d]) differ at the 0.05 level; [4] N.D. stands for not detected.

fucoidan derived from *Sargassum aquifolium* reported a marked increase in sulfate content accompanied by reductions in total sugar and fucose levels, indicating that sulfate substitution alters the native carbohydrate composition[11]. For sulfate content in Table 1, as expected, sulfate content increased markedly after oversulfation, confirming the successful incorporation of sulfate groups into SC-H_2O_2. These compositional changes highlight the need for further investigation into the biological functions of SC-H_2O_2-S1 and SC-H_2O_2-S2. The analysis of fucoidan's monosaccharide composition is critical, as fucoidans are chemically heterogeneous sulfated polysaccharides whose biological activities, including anticoagulant, antiviral, anti-inflammatory, and antioxidant effects, are highly dependent on their constituent sugars, their relative proportions (e.g., fucose, galactose, xylose, glucuronic acid), and their structural arrangements[17]. Variations in monosaccharide profiles have been associated with differences in bioactivity arising from species origin, harvest conditions, extraction and purification methods, and molecular weight fractions. Therefore, detailed compositional analysis is an essential component of any structure-activity relationship (SAR) investigation of fucoidan[21]. Furthermore, previous studies have also demonstrated that variations in fucose content and the presence of uronic acids or other neutral sugars can largely account for differences in the anticoagulant, antiviral, and immunomodulatory activities of fucoidans[27]. Table 1 summarizes the monosaccharide compositions of SC, SC-H_2O_2, SC-H_2O_2-S1, and SC-H_2O_2-S2. The primary monosaccharides in SC were fucose, galactose, glucuronic acid (GlcA), and galacturonic acid (GalA). Upon oxidative degradation, the molar ratios of GlcA and GalA decreased. Previous reports suggest that hydroxyl radicals and other reactive oxidants generated during H_2O_2/UV or Fenton-type treatments preferentially target electron-rich sites, oxidizing the carboxyl group (–COOH) and adjacent carbons of uronic acids. This oxidation can result in ring opening and decarboxylation (loss of CO_2) or formation of small oxidized fragments that are not detected as intact GlcA or GalA in monosaccharide assays[28]. Moreover, uronic acids are often located in side chains or linkages that are particularly susceptible to free-radical attack; oxidative cleavage can therefore release small acidic fragments or remove these residues preferentially from the polymer backbone, reducing their relative abundance in the recovered polysaccharide fraction[29]. Table 1 further indicates that following oversulfation (SC-H_2O_2-S1 and SC-H_2O_2-S2), glucuronic acid (GlcA) and galacturonic acid (GalA) became undetectable. Oversulfation methods, including chlorosulfonic acid–pyridine, SO_3–pyridine, or other sulfur trioxide complexes, primarily introduce sulfate esters on free hydroxyl groups, but under rigorous conditions they can also react with other nucleophilic sites, induce trans-esterification or ester formation at carboxylate centers, or generate mixed anhydrides. These chemical modifications alter the reactivity and derivatization behavior of formerly free carboxyl groups, rendering GlcA and GalA undetectable by assays that rely on the native uronic-acid structure[11]. Additionally, uronic acids located in labile positions, such as side chains or junctions, are preferentially removed during oxidative degradation; subsequent oversulfation primarily modifies the remaining backbone, which is largely composed of fucose and other neutral sugars, resulting in the absence of uronic residues in the final product[30]. Consequently, the sequential process of oxidative degradation followed by oversulfation simplifies the monosaccharide composition, reducing its complexity without introducing new monosaccharide species. Collectively, these results highlight notable differences in the monosaccharide compositions, particularly GlcA and GalA, among SC, SC-H_2O_2, SC-H_2O_2-S1, and SC-H_2O_2-S2, underscoring the necessity of further biological evaluations of these fucoidan derivatives.

Structural analyses of SC, SC-H_2O_2, SC-H_2O_2-S1, and SC-H_2O_2-S2

The infrared absorption bands observed at 3401 and 2940 cm^{-1} correspond to the O–H and H_2O stretching vibrations, as well as the C–H stretching associated with the pyranoid ring or the C-6 positions of fucose and galactose residues, respectively[16], as illustrated in Fig. 1. In typical polysaccharide structures, absorption signals at 1621 and 1421 cm^{-1} are attributed to H_2O scissoring and the in-plane vibrations involving CCH, COH, and OCH groups within the ring framework[16,31]. A distinct peak at 1230 cm^{-1} is linked to asymmetric S=O stretching within the ring or to C–O–H stretching related to the glycosidic bond[16]. The absorption peak at 1055 cm^{-1} can be attributed to C–O–C stretching vibrations within the pyranose ring or to C–O–H stretching

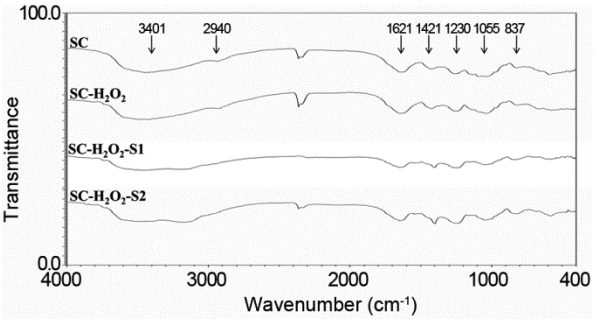

Fig. 1 — FTIR spectra for SC, SC-H_2O_2, SC-H_2O_2-S1, and SC-H_2O_2-S2. The characteristic peaks are labeled.

associated with the glycosidic bond[11]. Additionally, the band appearing at 837 cm^{-1} is indicative of equatorial C–O–S bending vibrations, associated with sulfate groups substituted at the axial C-4 position, likely on fucose[18]. Compared to SC and SC-H_2O_2, the absorption bands at 1230 cm^{-1} and 837 cm^{-1} were broader in the SC-H_2O_2-S1 and SC-H_2O_2-S2 fucoidan samples, indicating a higher sulfate content in these oversulfated derivatives. NMR analyses were also employed in this investigation to validate the distinct absorption of fucoidan extracts. The ^{1}H-NMR spectra of the fucoidan extracts are shown in Supplementary Fig. S2A. The L-fucopyranosyl units are in charge of the signals in the 5.5 to 5.0 ppm range[32]. A signal at 4.13 ppm (4[H]) is characteristic of a 3-linked α-L-fucose residue[31]. The presence of a (1→6)-β-D-galactan is suggested by the resonances at 4.07 and 3.95 ppm (6[H]/6′[H])[33]. Resonance signals within the 3.9–3.6 ppm range are likely associated with mannitol, a compound commonly co-extracted with fucoidan[34]. Additionally, peaks at 3.72 and 3.78 ppm correspond to (4[H]) 2,3-linked α- or β-mannose and (3[H]) 4-linked β-D-galactose, respectively[31]. Furthermore, the chemical shifts at 1.92 and 1.23 ppm are attributed to protons on sulfonyl-bound alkyl chains and methyl group protons from alkanes (often found in L-fucose), respectively[35]. The ^{13}C-NMR spectra of extracts of fucoidan are shown in Supplementary Fig. S2B. The presence of α-fucopyranosides is generally indicated by signals in the anomeric range of 97-102 ppm[36]. Furthermore, the signals ranging from 105 to 74 ppm indicate that the fucopyranose ring contains glycosylated or sulfated carbons. Signals ranging from 71 to 66 ppm are indicative of unsubstituted carbons[37]. A signal at 100.3 ppm indicates a (1,3)-linked α-L-fucopyranose residue[34]. There is (1-6)-β-D-linked galacton present when the peaks fall between 80 and 65 ppm[33]. Residues of β-D-galactopyranose are detected by signals at 66.34 and 62.88 ppm[38]. Analysis of the ^{1}H and ^{13}C NMR spectral data suggests that the polysaccharide possesses a backbone primarily composed of α-(1→3)-linked L-fucose residues, as evidenced by characteristic anomeric resonances (~5.0–5.5 ppm in ^{1}H and ~97–102 ppm in ^{13}C). This main chain is substituted with β-(1→6)-linked galactose side branches, supported by resonances at 4.07/3.95 ppm and carbon shifts between ~80–65 ppm. Resonances attributable to sulfated carbons (105–74 ppm) and sulfonyl-bound alkyl protons (~1.92 ppm), indicative of sulfate ester substitutions on sugar residues. SC and SC-H_2O_2 likely contain native sulfate esters predominantly at C-2 and/or C-4 positions of fucopyranose. SC-H_2O_2-S1 and SC-H_2O_2-S_2 have elevated sulfate contents, suggesting additional sulfate esterification at secondary hydroxyls on fucose and galactose units, potentially at C-3, C-4, and C-6 positions, increasing negative charge density and altering conformation. In addition, minor components such as mannose and mannitol were identified, along with terminal methyl and alkyl groups, which enhance the structural complexity and heterogeneity of the polysaccharide. Collectively, this data supports a branched fucoidan structure with an α-L-fucose main chain substituted with β-D-galactose and decorated with sulfate groups at multiple positions (likely C-2, C-3, and C-4 hydroxyl moieties of fucose and galactose rings), consistent with classical fucoidan structural motifs. The intensity and chemical shift distribution of sulfate-associated signals increase progressively from SC to SC-H_2O_2, SC-H_2O_2-S1, and SC-H_2O_2-S_2, indicating increasing degrees of sulfation. Previous studies have shown that the biological activities of oversulfated fucoidan derivatives can be detected, and their potency can probably be explained by the sulfate content differences[39,40]. The sulfate group has been successfully added to SC-H_2O_2-S1 and SC-H_2O_2-S2, as evidenced by composition and structure analyses. The anticancer efficacy of fucoidans is closely associated with their degree of sulfation, molecular weight, and monosaccharide composition. Highly sulfated fucoidans exhibit enhanced antiproliferative and pro-apoptotic activities across various cancer models. Sulfate groups increase negative charge density, facilitating interactions with growth factor receptors, integrins, and apoptosis-related proteins, which promotes caspase activation and suppresses

pro-survival signaling pathways such as PI3K/Akt and MAPK[26]. Increased sulfation also strengthens electrostatic binding to positively charged oncogenic proteins, including VEGF and EGFR, as well as extracellular matrix components, thereby inhibiting angiogenesis and metastatic progression[41]. Moreover, sulfation patterns and branching architectures influence conformational flexibility, receptor recognition, and cellular internalization. Fucoidans bearing sulfate substitutions at C-2, C-3, and C-4 positions generally display superior anticancer activity compared with less substituted counterparts[42]. Accordingly, the extensively sulfated derivatives SC-H_2O_2-S1 and SC-H_2O_2-S2 are expected to exhibit stronger anticancer effects than SC and SC-H_2O_2. In addition, sulfated fucoidans exert immunostimulatory effects by engaging pattern recognition receptors such as TLR2 and TLR4 on macrophages and dendritic cells, thereby activating NF-κB and MAPK signaling pathways and promoting cytokine secretion, phagocytosis, and immune cell activation. Higher sulfate densities further enhance macrophage and natural killer cell responses, supporting antitumor immunosurveillance. Medium- to low-molecular-weight, branched fucoidans may also improve immune cell communication and tumor penetration[40]. Based on these structure-activity relationships, the anticancer and immunomodulatory functions of SC-H_2O_2-S1 and SC-H_2O_2-S2 were further investigated. Because fucoidan is a high-molecular-weight polysaccharide with a highly complex and heterogeneous structure, its detailed elucidation remains challenging. From a future perspective, combining two-dimensional NMR techniques such as HSQC, COSY, and HMBC with conventional one-dimensional ^{1}H and ^{13}C NMR would markedly enhance structural resolution. Multidimensional NMR enables precise proton-carbon correlations, resolves signal overlap, and allows reliable assignment of glycosidic linkages, branching motifs, and substitution sites. Such approaches provide critical insights into how sulfation and depolymerization alter fucoidan structure and related biological functions[43].

The mitochondrial apoptotic pathway is involved in SC, SC-H_2O_2, SC-H_2O_2-S1, and SC-H_2O_2-S2-treated A-549 cells

The intrinsic mitochondria-dependent apoptotic pathway involves the loss of mitochondrial membrane potential (MMP), releasing cytochrome c, modulation of Bcl-2 and Bax expression levels, and forming an apoptotic complex in which caspases are activated.

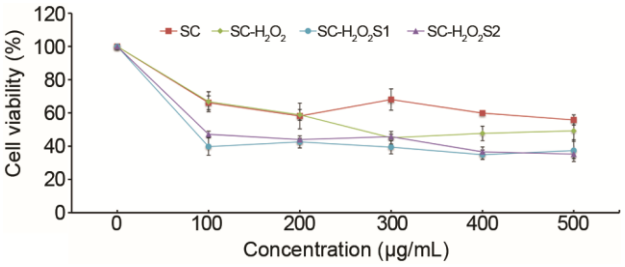

Fig. 2 — A-549 cell survival after SC, SC-H_2O_2, SC-H_2O_2-S1, and SC-H_2O_2-S2 treatments. Cell viability was evaluated after 48 h of treatment with SC, SC-H_2O_2, SC-H_2O_2-S1, and SC-H_2O_2-S2 (0–500 μg/mL). Data are presented as the mean with standard deviation (n = 3).

Among these events, the decline in MMP is considered an early indicator of apoptotic initiation[44]. Recent studies demonstrate that highly sulfated polysaccharides exhibit pronounced anti-lung cancer activity. A sulfated fraction (N50 F2) from *Antrodia cinnamomea* with a sulfate content of 3.89 mmol/g markedly inhibited lung cancer cell proliferation and migration by suppressing AKT, ERK, EGFR, and FAK signaling, downregulating metastasis-related factors, and activating apoptotic pathways[45]. Similarly, chemically sulfated *Zizania latifolia* polysaccharides showed enhanced cytotoxicity toward A549 cells, with SZLP-2 (with a degree of substitution approximately 15.1 ± 2.50) displaying the strongest antiproliferative effect[46]. Collectively, these findings support the potential of oversulfated fucoidan as an effective anti-lung cancer agent. The present study evaluated the effects of SC, SC-H_2O_2, SC-H_2O_2-S1, and SC-H_2O_2-S2 on A-549 cells' apoptotic factors. Initially, we examined the cytotoxic effects of SC, SC-H_2O_2, SC-H_2O_2-S1, and SC-H_2O_2-S2 on A-549 cells. As seen in Fig. 2, after 48 h of treatment with 0–500 μg/mL of SC, SC-H_2O_2, SC-H_2O_2-S1, and SC-H_2O_2-S2, the vitality of A-549 cells declined in response to the progressively higher concentrations of the fucoidan samples. After subjecting A-549 cells to 200 μg/mL fucoidan extracts for 48 h, the cells' viability was reduced, and, in general, the value approached the reaction plateau. Therefore, for additional cellular experiments, a concentration of 200 μg/mL fucoidan extracts and a 48h treatment duration were employed. Further, the MMP loss was evaluated using a fluorescent dye, TMRE. Table 2 illustrates that after 48 h of exposure to 200 μg/mL of SC, SC-H_2O_2, SC-H_2O_2-S1, and SC-H_2O_2-S2, A-549 cells showed a statistically significant increase in low MMP cells in comparison to the untreated group. The most significant MMP loss was caused by SC-H_2O_2-

S1, suggesting that MMP loss in A-549 cells can be potently induced by moderately oversulfated fucoidan (SC-H_2O_2-S1). It has been documented that the Bcl-2 proteins prevent MMP depolarization and impede cytochrome c, apoptosis-inducing factor (AIF), and Smac/Diablo activation[47]. Table 2 displays the results of an examination of the effects of SC, SC-H_2O_2, SC-H_2O_2-S1, and SC-H_2O_2-S2 on Bcl-2 expression in A-549 cells. After subjecting A-549 cells to 200 μg/mL of SC, SC-H_2O_2, SC-H_2O_2-S1, and SC-H_2O_2-S2 for 48 h, there was a statistically significant decrease in the amount of Bcl-2 compared to the untreated control. Out of all the fucoidan extracts, SC-H_2O_2-S2 had the highest level of Bcl-2 suppression, indicating that fucoidan oversulfation has a strong effect on suppressing Bcl-2 expression in A-549 cells when compared to SC. Furthermore, it has been shown that Bax, a member of the Bcl-2 family proteins, activates a number of downstream death effectors[48]. Table 2 presents the results of an examination of the effects of SC, SC-H_2O_2, SC-H_2O_2-S1, and SC-H_2O_2-S2 on Bax expression in A-549 cells. When A-549 cells were exposed to 200 μg/mL of SC, SC-H_2O_2, SC-H_2O_2-S1, and SC-H_2O_2-S2 for 48 h, there was a statistically significant increase in the amount of Bax in the cells compared to the untreated control. Among these fucoidan extracts, SC-H_2O_2-S1 exhibited the greatest induction of Bax, suggesting that the oversulfation of fucoidan has potent activity in activating Bax expression in A-549 cells compared with SC. As suggested by previous studies, a decrease in MMP causes matrix condensation, which easily leads to cytochrome c release and apoptosis[49]. Here, we examined the extent to which SC, SC-H_2O_2, SC-H_2O_2-S1, and SC-H_2O_2-S2 affected the release of cytochrome c in A-549 cells, and the corresponding results are displayed in Table 2. After subjecting A-549 cells to 200 μg/mL of SC, SC-H_2O_2, SC-H_2O_2-S1, and SC-H_2O_2-S2 for 48 h, there was a statistically significant decrease in the number of cells with a high fluorescence level of cytochrome c as compared to the untreated control. Following the release of cytochrome c from the mitochondrial intermembrane space, an apoptosome is assembled, subsequently initiating the activation of caspase-9, followed by caspase-8 and caspase-3[47]. In the present study, the effects of SC, SC-H_2O_2, SC-H_2O_2-S1, and SC-H_2O_2-S2 on the activation of these caspases were examined in A-549 cells. As presented in Table 2, treatment with 200 μg/mL of each compound for 48 h led to a statistically significant elevation in the levels of active caspase-9, -8, and -3, when compared with the untreated group. A flow-cytometric Annexin V/PI analysis was utilized to identify the apoptosis of cells following treatments with SC, SC-H_2O_2, SC-H_2O_2-S1, and SC-H_2O_2-S2 in order to further corroborate the apoptotic patterns of cells. The data shown in Fig. 3 indicate that in SC-H_2O_2-S1 and SC-H_2O_2-S2-induced cell death, late apoptosis of cells is predominant. In the untreated control group, the proportion of viable A-549 cells was 68.3% ± 0.6%, indicating that 48 h of nutrient deprivation alone induced a certain degree of apoptosis and necrosis. In earlier studies on anti-lung cancer activity, treatment with fucoidan extracted from *Padina distromatica* at a concentration of 1000 μg/mL for 48 h resulted in an A-549 cell viability of approximately 65.44% ± 1.35%[50]. As demonstrated in Fig. 3B, treatment of A-549 cells at 200 μg/mL for 48 h resulted in survival rates of 4.80±0.43 % and 4.33±0.33 %, respectively, indicating a substantially stronger cytotoxic effect of SC-H_2O_2-S1 and SC-H_2O_2-S2 compared to fucoidan from *P. distromatica*. According to previous investigations, after treating A-549 cells with the fucoidan isolated from *Turbinaria conoides* at 250 μg/mL for 72 h, a survival rate of about 35% of the cells was found[51]. Similarly, Fig 3B demonstrated that SC-H_2O_2-S1 and SC-H_2O_2-

Table 2 — Expressions of mitochondria-dependent apoptotic factors in SC-, SC-H_2O_2-, SC-H_2O_2-S1-, and SC-H_2O_2-S2-treated A549 cells. A-549 cells were exposed without or with to SC, SC-H_2O_2, SC-H_2O_2-S1, and SC-H_2O_2-S2 at a dose of 200 μg/mL for 48 h.

Factors	Control	SC	SC-H_2O_2	SC-H_2O_2-S1	SC-H_2O_2-S2
Low mitochondrial membrane potential (%)[1]	22.4 ± 0.3 [a]	38.6 ± 0.6 [c]	36.4 ± 0.7 [b]	70.7 ± 0.40 [e]	62.2 ± 1.1 [d]
Level of Bcl-2 (%) [1]	61.0 ± 0.5 [e]	51.9 ± 0.2 [d]	45.7 ± 0.4 [b]	49.9 ± 0.5 [c]	34.7 ± 0.6 [a]
Level of Bax (%) [1]	16.1 ± 0.2 [a]	26.3 ± 0.4 [b]	28.6 ± 0.3 [c]	36.7 ± 0.4 [e]	31.7 ± 0.5 [d]
Release of cytochrome c (%) [1]	96.0 ± 0.1 [c]	92.5 ± 0.3 [b]	91.5 ± 0.1 [a]	93.3 ± 0.2 [b]	93.1 ± 0.1 [b]
Caspase-9 activity (%) [1]	39.2 ± 0.4 [a]	47.0 ± 0.3 [c]	51.9 ± 0.2 [d]	42.4 ± 0.7 [b]	42.8 ± 0.1 [b]
Caspase-8 activity (%) [1]	38.9 ± 0.3 [a]	56.9 ± 0.2 [d]	67.7 ± 0.3 [e]	46.2 ± 0.5 [b]	52.9 ± 0.3 [c]
Caspase-3 activity (%) [1]	39.5 ± 0.2 [a]	49.3 ± 0.2 [b]	61.5 ± 0.4 [d]	50.6 ± 0.4 [c]	50.5 ± 0.6 [bc]

[1]Triplicate experiment was conducted; results within the same row differ at the 0.05 level for letters ([a], [b], [c], [d], [e]).

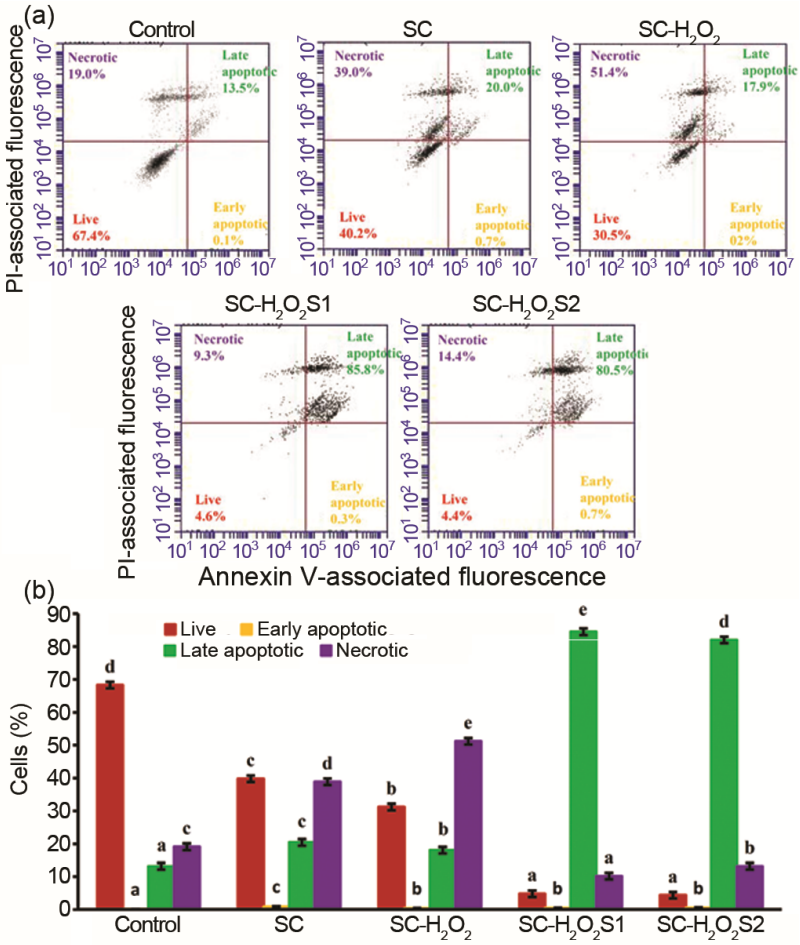

Fig. 3 — SC, SC-H_2O_2, SC-H_2O_2-S1, and SC-H_2O_2-S2 cause apoptosis of A-549 cells. (a) Flow cytometric charts of annexin V-FITC/PI-stained A-549 cells treated with and without 200 μg/mL SC, SC-H_2O_2, SC-H_2O_2-S1, and SC-H_2O_2-S2 for 48 h; and (b) a bar graph that displays the percentages of living, early apoptotic, late apoptotic, and necrotic cells, summarizing the results of the three independent cell cytometry experiments. There is a significant difference at the 0.05 level for bars with different lettering (a, b, c, d, e).

S2 had a significantly more cytotoxic effect on A-549 cells than that of *T. conoides* fucoidan. These data suggest that SC-H_2O_2-S1 and SC-H_2O_2-S2 may be good anti-lung cancer candidates compared to other reported data. In summary, treatments with SC, SC-H_2O_2, SC-H_2O_2-S1, and SC-H_2O_2-S2 triggered apoptosis in A-549 cells through multiple mechanisms, including disruption of mitochondrial membrane potential, downregulation of Bcl-2, upregulation of Bax, enhanced release of cytochrome c, increased activation of caspases-9, -8, and -3, and a rise in late-stage apoptotic cell populations. Overall, the oversulfated fucoidan derivatives demonstrated stronger pro-apoptotic activity compared to SC and SC-H_2O_2, highlighting their promise as candidates for preventive or adjunctive therapies in lung cancer treatment.

SC, SC-H_2O_2, SC-H_2O_2-S1, and SC-H_2O_2-S2 inhibited cell migration by modulating RANK and MMP9 expressions in A-549 cells

Tumor cell migration is closely linked to the activity of matrix metalloproteinases (MMPs), which facilitate the breakdown of extracellular matrix (ECM) components. Among them, matrix metalloproteinase-9 (MMP-9) is widely present in human tissues, serum, and urine, and has been associated with the progression of muscle-invasive conditions[52]. Additionally, the RANK/RANKL pathway plays a role in MMPs activation. Previous studies have demonstrated that RANKL binding to RANK on osteoclasts, mediated by osteoblasts, and then initiates transcriptional regulators. It also promotes the production of enzymes such as cathepsin K and MMP-9 and activates downstream signaling pathways[53]. As shown in Fig. 4, treatment of A-549

cells with 200 µg/mL of SC, SC-H_2O_2, SC-H_2O_2-S1, and SC-H_2O_2-S2 for 48 h led to a statistically significant decline in cell migration compared to the control group. In additional experiments, we evaluated the expressions of RANK and MMP-9 in SC-, SC-H_2O_2-, SC-H_2O_2-S1-, and SC-H_2O_2-S2-treated A549 cells, and the results are shown in Table 3. A statistically significant reduction of RANK and MMP-9 expressions was detected in A-549 cells following exposure to SC, SC-H_2O_2, SC-H_2O_2-S1, and SC-H_2O_2-S2 at a dose of 200 µg/mL for 48 h, as compared to the untreated group. These data elucidate that SC, SC-H_2O_2, SC-H_2O_2-S1, and SC-H_2O_2-S2 can eliminate A-549 cell migration by modulating the expressions of RANK and MMP-9. However, additional *in vivo* research is essential to provide a detailed overview of the signaling cascade. To validate the anti-migration and anti-metastatic effects observed in A-549 cells, appropriate *in vivo* models include orthotopic lung cancer xenografts, in which human NSCLC cells (e.g., A-549) are implanted into the lung parenchyma or bronchus of immunodeficient mice. This model closely mimics the lung tumor microenvironment, invasion, and metastatic behavior. Patient-derived xenograft (PDX) models may further enhance clinical relevance by preserving tumor heterogeneity. In addition, experimental metastasis models using tail-vein or intracardiac injection of A-549 cells enable quantitative assessment of lung and distant organ colonization, with particular relevance to MMP-9-dependent early metastatic events. Key evaluation endpoints may include primary tumor growth assessed by imaging or caliper measurements, metastatic burden and nodule quantification by histopathology, and molecular analyses of RANK/RANKL and MMP-9 expression and activity using IHC, immunoblotting, zymography, or ELISA to elucidate the underlying mechanisms[54,55].

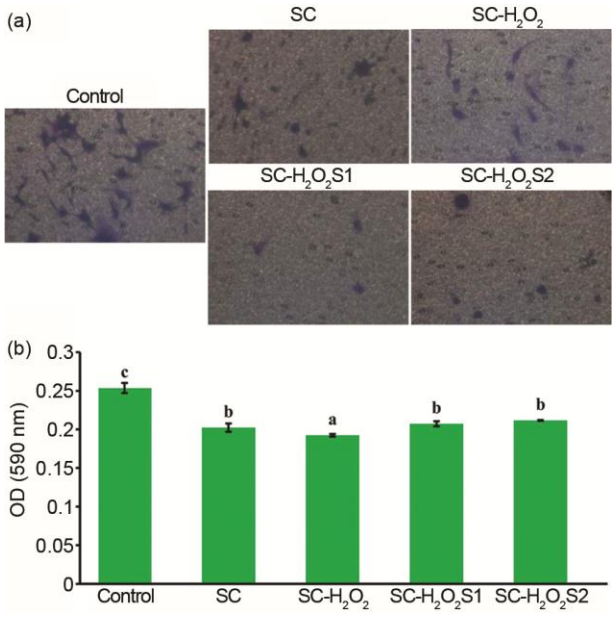

Fig. 4 — Patterns of cell migration in A549 cells treated with SC, SC-H_2O_2, SC-H_2O_2-S1, and SC-H_2O_2-S2. (a) A-549 cells were subjected to a 48-hour transwell analysis with and without 200 µg/mL SC, SC-H_2O_2, SC-H_2O_2-S1, and SC-H_2O_2-S2; (b) a bar graph summarizing the results of the three separate transwell investigations. Bars with distinct letter designations (^{a}, ^{b}, ^{c}) exhibit significant differences at the 0.05 level.

SC, SC-H_2O_2, SC-H_2O_2-S1, and SC-H_2O_2-S2 exhibited immunostimulant effects in RAW 264.7 cells

Nitric oxide (NO) functions as an inflammatory mediator, with its production stimulated by inflammatory cytokines or bacterial lipopolysaccharides (LPS) in various cell types, including macrophages[56]. Previous research has demonstrated that fucoidan can enhance the production of pro-inflammatory cytokines[57]. For instance, Tabarsa *et al*.[58] investigated the effects of fucoidan extracted from *Nizamuddinia zanardinii* on RAW 264.7 murine macrophages and NK-92 cells. A specific fraction of this brown seaweed extract showed notable immunostimulatory properties, increasing the release of NO, TNF-α, IL-1β, and IL-6. Additionally, it activated NF-κB, natural killer (NK) cells, and MAPK signaling pathways, which resulted in elevated levels of IFN-γ and TNF-α. Further studies revealed that fucoidan obtained from *Ascophyllum nodosum* and *Fucus vesiculosus* stimulates NO and cytokine production in RAW 264.7 cells by triggering the NF-κB and AP-1 pathways[59]. These results imply that the immunostimulatory effects of fucoidan may be associated with the selective activation of TLR-2 or TLR-4 receptors, leading to downstream activation of

Table 3 — Expressions of RANK/MMP-9 signaling factors in SC-, SC-H_2O_2-, SC-H_2O_2-S1-, and SC-H_2O_2-S2-treated A549 cells. A-549 cells were exposed without or with to SC, SC-H_2O_2, SC-H_2O_2-S1, and SC-H_2O_2-S2 at a dose of 200 µg/mL for 48 h.

Factors	Control	SC	SC-H_2O_2	SC-H_2O_2-S1	SC-H_2O_2-S2
RANK (%) [1]	73.5 ± 0.6 ^{d}	62.0 ± 0.1 ^{c}	61.7 ± 0.1 ^{c}	53.5 ± 1.3 ^{a}	58.8 ± 0.3 ^{b}
MMP-9 (%) [1]	81.5 ± 0.1 ^{e}	73.4 ± 0.4 ^{d}	65.3 ± 0.2 ^{b}	61.1 ± 0.2 ^{a}	66.2 ± 0.5 ^{c}

[1]Triplicate experiment was conducted; results within the same row differ at the 0.05 level for letters (^{a}, ^{b}, ^{c}, ^{d}, ^{e}).

NF-κB or MAPK signaling cascades and enhanced secretion of IL-6, IL-8, IL-1β, NO, TNF-α, and IFN-γ, depending on the species of brown algae examined[57]. Moreover, sulfate-modified fucoidan, a chemically enhanced derivative of the naturally occurring sulfated polysaccharide, has demonstrated potent immunostimulatory properties. Structural modifications, particularly increased sulfation, significantly influence fucoidan's biological activity by enhancing its interactions with pattern recognition receptors such as toll-like receptors (TLRs) and scavenger receptors. Studies have shown that sulfate-rich fucoidan can activate macrophages, dendritic cells, and natural killer (NK) cells, resulting in elevated secretion of pro-inflammatory cytokines, including IL-6, TNF-α, and IFN-γ, thereby promoting both innate and adaptive immune responses[40]. Studies have further confirmed that sulfate modification not only increases fucoidan's binding affinity to immune cell surface molecules but also enhances its potential as an immunotherapeutic adjuvant[40]. Additionally, emerging evidence indicates that the degree and position of sulfation critically determine fucoidan's immunomodulatory potency, providing a rationale for targeted structural modifications to optimize its bioactivity[57,60]. In the present study, the effects of SC, SC-H_2O_2, SC-H_2O_2-S1, and SC-H_2O_2-S2 on macrophage function were investigated using RAW 264.7 cells. Cell viability was assessed following exposure to these treatments. As shown in Table 4, cell viability remained high after SC treatment (100.1 ± 0.4%), comparable to the untreated control (100.0 ± 3.7%), indicating no cytotoxicity. In contrast, LPS treatment reduced cell viability to 88.5 ± 7.1%. Treatments with SC-H_2O_2 (85.1 ± 0.4%), SC-H_2O_2-S1 (86.1 ± 5.8%), and SC-H_2O_2-S2 (90.5 ± 3.0%) also resulted in slightly decreased viability compared to the control; however, all values remained within a viable range (85.1–100.1%). Regarding NO production, LPS stimulation markedly increased NO levels to 22.0 ± 0.5 μM compared to the control (7.7 ± 0.1 μM, $P < 0.05$). SC treatment further elevated NO levels to 33.2 ± 0.6 μM, indicating strong pro-inflammatory activation of macrophages. In contrast, SC-H_2O_2 caused only a moderate increase (9.8 ± 0.5 μM), close to basal levels. SC-H_2O_2-S1 and SC-H_2O_2-S2 induced NO production of 25.5 ± 1.0 μM and 15.3 ± 0.2 μM, respectively, both significantly higher than SC-H_2O_2 ($P < 0.05$). These findings suggest that the molecular structure of fucoidan, including its degree of degradation and sulfation, critically influences macrophage activation. Higher sulfation of fucoidan appears to modulate NO production, potentially due to altered interactions with cellular receptors or signaling pathways, as previously reported by Jayawardena *et al.*[6]. The reduced NO production by degraded fucoidan (SC-H_2O_2) suggests potential anti-inflammatory properties, consistent with previous findings that lower molecular weight fucoidans exhibit distinct biological activities[40]. Structural modifications may therefore be strategically employed to optimize fucoidan's therapeutic potential based on the desired immunomodulatory effect. The expression of inflammatory mediators iNOS and COX-2 was also evaluated (Table 4). LPS treatment significantly increased iNOS (58.2 ± 0.6%) and COX-2 (59.3 ± 0.3%) expression compared to the control group (iNOS: 49.9 ± 0.6%; COX-2: 51.4 ± 0.9%). SC treatment similarly elevated iNOS (56.0 ± 0.6%) and COX-2 (57.3 ± 0.5%). SC-H_2O_2 treatment resulted in greater suppression of both markers (iNOS: 52.6 ± 0.2%; COX-2: 53.4 ± 0.3%), suggesting enhanced anti-inflammatory activity due to molecular weight reduction. Furthermore, SC-H_2O_2-S1 increased the expression of iNOS (54.3 ± 0.1%) and COX-2 (55.2 ± 0.1%) compared to SC-H_2O_2, indicating that moderate sulfation may enhance the pro-inflammatory

Table 4 — Expression of immunostimulatory factors in RAW 264.7 cells treated with SC, SC-H_2O_2, SC-H_2O_2-S1, and SC-H_2O_2-S2. RAW 264.7 cells were treated with SC, SC-H_2O_2, SC-H_2O_2-S1, or SC-H_2O_2-S2 at a concentration of 500 μg/mL for 24 hours. Cells treated with 1 μg/mL LPS served as a positive control

Factors	Control	LPS	SC	SC-H_2O_2	SC-H_2O_2-S1	SC-H_2O_2-S2
Cell viability (%) [1]	100.0 ± 3.7 [b]	88.5 ± 7.1 [a]	100.1 ± 0.4 [b]	85.1 ± 0.4 [a]	86.1 ± 5.8 [a]	90.5 ± 3.0 [a]
NO (μM) [1]	7.7 ± 0.1 [a]	22.0 ± 0.5 [d]	33.2 ± 0.6 [f]	9.8 ± 0.5 [b]	25.5 ± 1.0 [e]	15.3 ± 0.2 [c]
iNOS (%) [1]	49.9 ± 0.6 [a]	58.2 ± 0.6 [e]	56.0 ± 0.6 [d]	52.6 ± 0.2 [b]	54.3 ± 0.1 [c]	52.9 ± 0.3 [b]
COX-2 (%) [1]	51.4 ± 0.9 [a]	59.3 ± 0.3 [e]	57.3 ± 0.5 [d]	53.4 ± 0.3 [b]	55.2 ± 0.1 [c]	53.3 ± 0.2 [b]
TNF-α (pg/mL) [1]	126.9 ± 12.6 [a]	3753.1 ± 36.9 [d]	3690.3 ± 39.9 [d]	1233.2 ± 6.7 [b]	1725.0 ± 41.6 [c]	1276.3 ± 41.8 [b]
IL-6 (pg/mL) [1]	2.2 ± 1.6 [a]	2493.5 ± 16.3 [d]	1212.6 ± 19.1 [c]	68.2 ± 2.5 [b]	80.0 ± 2.6 [b]	58.2 ± 4.1 [b]
IL-1β (pg/mL) [1]	80.7 ± 24.9 [a]	894.0 ± 43.2 [f]	700.7 ± 24.9 [e]	300.7 ± 52.5 [b]	547.3 ± 41.1 [d]	427.3 ± 18.9 [c]

[1]Triplicate experiment was conducted; results within the same row differ at the 0.05 level for letters ([a], [b], [c], [d], [e], [f]).

properties of fucoidan. However, excessive sulfation (SC-H_2O_2-S2) did not yield further enhancement. The effects of fucoidan and its derivatives on pro-inflammatory cytokine production (TNF-α, IL-6, and IL-1β) were also assessed (Table 4). As expected, LPS stimulation markedly increased TNF-α (3753.1 ± 36.9 pg/mL), IL-6 (2493.5 ± 16.3 pg/mL), and IL-1β (894.0 ± 43.2 pg/mL) compared to the untreated control group (TNF-α: 126.9 ± 12.6 pg/mL; IL-6: 2.2 ± 1.6 pg/mL; IL-1β: 80.7 ± 24.9 pg/mL). SC treatment also significantly increased TNF-α (3690.3 ± 39.9 pg/mL), IL-6 (1212.6 ± 19.1 pg/mL), and IL-1β (700.7 ± 24.9 pg/mL). In contrast, degraded fucoidan (SC-H_2O_2) markedly decreased the production of these cytokines (TNF-α: 1233.2 ± 6.7 pg/mL; IL-6: 68.2 ± 2.5 pg/mL; IL-1β: 300.7 ± 52.5 pg/mL), highlighting its potential anti-inflammatory activity. SC-H_2O_2-S1 partially restored cytokine levels (TNF-α: 1725.0 ± 41.6 pg/mL; IL-6: 80.0 ± 2.6 pg/mL; IL-1β: 547.3 ± 41.1 pg/mL) compared to SC-H_2O_2, indicating that moderate sulfation enhances pro-inflammatory activity, whereas excessive sulfation (SC-H_2O_2-S2) does not provide additional benefits. In summary, the data presented in Table 4 suggest that both molecular weight and controlled sulfation are critical in regulating the pro-inflammatory activity of fucoidan derivatives. SC demonstrates strong pro-inflammatory activity. When its molecular weight is reduced (SC-H_2O_2), this activity diminishes. Moderate sulfation of SC-H_2O_2 (SC-H_2O_2-S1) restores and enhances its pro-inflammatory effects, while excessive sulfation (SC-H_2O_2-S2) offers no further advantage. These findings highlight the potential of structurally modified fucoidan as a therapeutic candidate for managing inflammatory diseases.

Principal component analysis (PCA) and hierarchical clustering analysis (HCA)

The above findings characterize the compositional properties of four fucoidan derivatives (SC, SC-H_2O_2, SC-H_2O_2-S1, and SC-H_2O_2-S2) and highlight their varying anti-proliferative effects on A-549 cells as well as immunostimulatory effects on RAW 264.7 cells. Principal component analysis (PCA) was further employed to elucidate the relationships among variables and samples, while simultaneously transforming the complex dataset into a more interpretable chemometric space. The first two principal components (PC1 and PC2) explained 89.8% of the total data variance, with PC1 accounting for 45.3% and PC2 for 44.5%, indicating strong model reliability as the combined variance exceeded the 85% threshold[61]. In the PCA plot (Fig. 5A), TNF-α production, COX-2 expression, iNOS expression, IL-6 production, fucose content, NO production, and IL-1β production contributed more prominently to PC1, suggesting that PC1 is primarily associated with immune-enhancing characteristics in RAW 264.7 cells, with fucose content also playing a role in these properties. Conversely, caspase-8 activity, cytochrome c release, caspase-9 activity, low mitochondrial membrane potential, cell viability, cell migration, RANK expression, caspase-3 activity, Bax expression, and sulfate content contributed more significantly to PC2, indicating that PC2 reflects anti-proliferative factors in A549 cells, with sulfate content also involved in anti-proliferative properties. Furthermore, the PCA plot (Fig. 5A) shows that SC is closely associated with IL-6 production, TNF-α production, COX-2 expression, iNOS expression, fucose content, NO production, and IL-1β production.

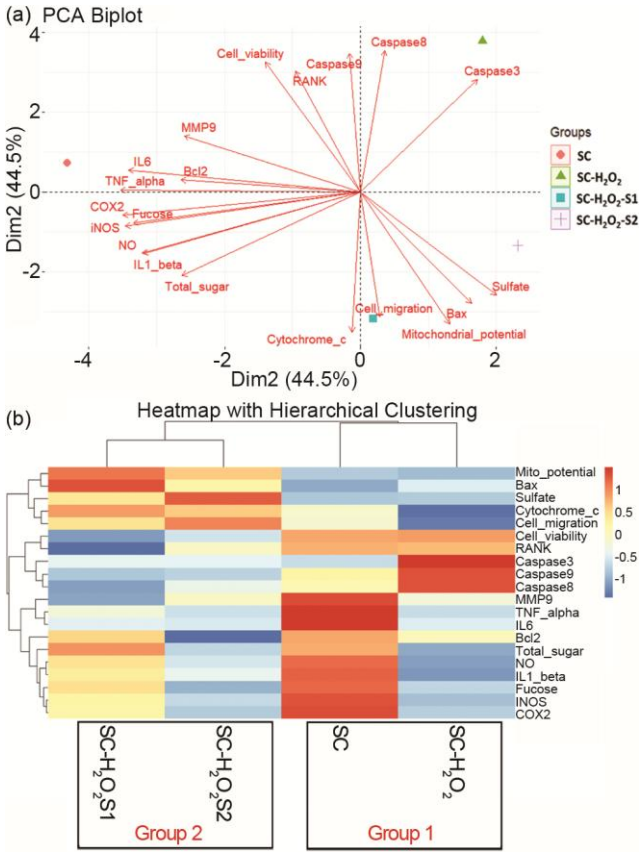

Fig. 5 — (a) Principal component analysis plot and (b) hierarchical cluster analysis and heatmap plot of chemical analyses, apoptosis parameters, and immunostimulant factors derived from SC, SC-H_2O_2, SC-H_2O_2-S1, and SC-H_2O_2-S2.

SC-H_2O_2 is positioned near caspase-9, -8, and -3 activities, while SC-H_2O_2-S1 is located closer to cytochrome c release, cell migration, low mitochondrial membrane potential, and Bax expression. SC-H_2O_2-S2 is situated near sulfate content, Bax expression, and low mitochondrial membrane potential. Notably, there is no obvious overlap among the data clusters for SC, SC-H_2O_2, SC-H_2O_2-S1, and SC-H_2O_2-S2, indicating a high degree of data dispersion and clear differentiation among the groups[62]. These findings suggest that the fucoidan derivatives have significant effects on chemical composition, anti-proliferative activity in A549 cells, and immune-enhancing effects in RAW 264.7 cells. To further elucidate the relationships among SC, SC-H_2O_2, SC-H_2O_2-S1, SC-H_2O_2-S2, and the related factors, hierarchical clustering analysis (HCA) and a heatmap plot were performed. In this approach, samples that clustered together exhibited similar characteristics and shared distinct features representative of their respective groups. As shown in Fig. 5B, SC clustered with SC-H_2O_2 to form Group 1, while SC-H_2O_2-S1 clustered with SC-H_2O_2-S2 to form Group 2. Notably, the degree of similarity within Group 1 was lower than that observed within Group 2. Interestingly, fucose content was closely associated with iNOS and COX-2 expression, suggesting that fucose may play a role in regulating the expression of these inflammatory mediators. Moreover, total sugar content was located near NO, IL-1β, fucose, iNOS, and COX-2. Sulfate content was found to be closely associated with cytochrome c release and cell migration. The chemical compositions, anti-proliferative factors in A549 cells, and immune-enhancing factors in RAW 264.7 cells measured in the present study included 20 variables. The correlations among the samples and variables were illustrated in a heatmap (Fig. 5B). It was shown that MMP-9, TNF-α, IL-6, NO, IL-1β, fucose, iNOS, and COX-2 were positively correlated with SC; caspase-3, caspase-9, and caspase-8 were positively correlated with SC-H_2O_2; low mitochondrial membrane potential and Bax expression were positively correlated with SC-H_2O_2-S1; and sulfate content and cell migration were positively correlated with SC-H_2O_2-S2. Collectively, the integration of PCA, HCA, and heatmap analyses revealed that Group 1 (SC and SC-H_2O_2) was characterized by modulation of apoptosis and immune-enhancing factors, whereas Group 2 (SC-H_2O_2-S1 and SC-H_2O_2-S2) exhibited stronger associations with apoptosis and cell migration.

Conclusion

This study successfully derived four distinct fucoidans (SC, SC-H_2O_2, SC-H_2O_2-S1, and SC-H_2O_2-S2) from extrusion-pretreated *S. crassifolium*. These fucoidans exhibited varying chemical compositions and structural characteristics. *In vitro* assessments demonstrated the apoptotic effects of SC, SC-H_2O_2, SC-H_2O_2-S1, and SC-H_2O_2-S2 on A-549 cells. Notably, SC-H_2O_2-S1 displayed the most potent anti-lung cancer properties, indicating its potential as a promising adjuvant treatment for lung cancer. Furthermore, these fucoidans exhibited the ability to inhibit the migration of lung cancer cells by modulating the expressions of RANK and MMP-9. Immunostimulant analyses revealed that these fucoidan derivatives enhanced pro-inflammatory properties. In general, SC-H_2O_2 exhibited lower immunostimulant activity compared to SC. However, SC-H_2O_2-S1 showed increased immunostimulant properties relative to SC-H_2O_2. These findings suggest that adjusting the molecular weight and sulfate content of fucoidan can modify its pro-inflammatory activity and overall bioactive functions. Integrated analyses using PCA, HCA, and heatmap visualization revealed distinct bioactivity profiles between the two groups. Group 1, comprising SC and SC-H_2O_2, was primarily associated with the regulation of apoptotic pathways and immune-enhancing responses. In contrast, Group 2, consisting of SC-H_2O_2-S1 and SC-H_2O_2-S2, demonstrated stronger correlations with both apoptotic signaling and cell migration processes. Further investigations are warranted to comprehensively elucidate the underlying signaling mechanisms, with emphasis on conducting *in vivo* studies.

Funding statement

This research was funded by Yuan's General Hospital, Taiwan, grant number YUAN-IACR-23-01 to Wei-Cheng Hsiao. This work was supported by grants from the Kaohsiung Medical University Hospital (KMUH112-M201) to Tien-Chiu Wu. This work was supported by the National Science and Technology Council, Taiwan [grant number NSTC 113-2221-E-992-008], [grant number NSTC 114-2918-I-992-003], and [grant number NSTC 114-2221-E-992-020-MY3], which were awarded to Chun-

Yung Huang. This research was also supported by the Fishery Agency, Ministry of Agriculture, Taiwan, under grant number 113AS-6.3.2-FA-03 and 114AS-1.6.2-AS-24 which was awarded to Chun-Yung Huang.

Conflict of interest:

The authors declare that there are no conflicts of interest.

References

1 Siegel RL, Miller KD & Jemal A, Cancer statistics, 2017. *CA Cancer J Clin*, 67 (2017) 7.
2 Warrick KA, Vallez CN, Meibers HE & Pasare C, Bidirectional communication between the innate and adaptive immune systems. *Annu Rev Immunol*, 43 (2025) 489.
3 Mamilos A, Winter L, Schmitt VH, Barsch F, Grevenstein D, Wagner W, Babel M, Keller K, Schmitt C & Gürtler F, Macrophages: From simple phagocyte to an integrative regulatory cell for inflammation and tissue regeneration-a review of the literature. *Cells*, 12 (2023) 276.
4 Kim ME & Lee JS, Advances in the regulation of inflammatory mediators in nitric oxide synthase: Implications for disease modulation and therapeutic approaches. *Int J Mol Sci*, 26 (2025) 1204.
5 Ciesielska A, Matyjek M & Kwiatkowska K, TLR4 and CD14 trafficking and its influence on LPS-induced pro-inflammatory signaling. *Cell Mol Life Sci*, 78 (2021) 1233.
6 Jayawardena TU, Nagahawatta DP, Fernando I, Kim YT, Kim JS, Kim WS, Lee JS & Jeon YJ, A review on fucoidan structure, extraction techniques, and its role as an immunomodulatory agent. *Mar Drugs*, 20 (2022) 755.
7 Fagundo-Mollineda A, Freile-Pelegrín Y, Vásquez-Elizondo RM, Vázquez-Delfín E & Robledo D, *Sargassum*: Turning coastal challenge into a valuable resource. *Biomass*, 6 (2026) 9.
8 Huang CY, Wu SJ, Yang WN, Kuan AW & Chen CY, Antioxidant activities of crude extracts of fucoidan extracted from *Sargassum glaucescens* by a compressional-puffing-hydrothermal extraction process. *Food Chem*, 197 (2016) 1121.
9 Zhou R, Zhong L, Jia S, Luo Y, Li Y & Tang Y, Preparation and characterization of aspirin–fucoidan complex and its admirable antitumor activity on human non-small cell lung cancer cells. *Int J Biol Macromol*, 263 (2024) 130163.
10 Huang CY, Kuo CH & Lee CH, Antibacterial and antioxidant capacities and attenuation of lipid accumulation in 3T3-L1 adipocytes by low-molecular-weight fucoidans prepared from compressional-puffing-pretreated *Sargassum crassifolium*. *Mar Drugs*, 16 (2018) 24.
11 Hsiao HH, Wu TC, Tsai YH, Kuo CH, Huang RH, Hong YH & Huang CY, Effect of oversulfation on the composition, structure, and *in vitro* anti-lung cancer activity of fucoidans extracted from *Sargassum aquifolium*. *Mar Drugs*, 19 (2021) 215.
12 Ali IM, Forsido SF, Kuyu CG, Ahmed EH, Andersa KN, Chane KT & Regasa TK, Effects of extrusion process conditions on nutritional, anti-nutritional, physical, functional, and sensory properties of extruded snack: A review. *Food Sci Nutr*, 12 (2024) 8755.
13 Yadav N, Suvedi D, Sharma A, Khanal S, Verma R, Kumar D, Khan Z & Peter L, Extrusion technology in food processing: Principles, innovations and applications in sustainable product development. *Food Humanit*, 5 (2025) 100672.
14 Xu Y, Jia F, Wu Y, Jiang J, Zheng T, Zheng H & Yang Y, The impact of extrusion cooking on the physical properties, functional components, and pharmacological activities of natural medicinal and edible plants: A Review. *Foods*, 14 (2025) 1869.
15 Hsiao WC, Hong YH, Tsai YH, Lee YC, Patel AK, Guo HR, Kuo CH & Huang CY, Extraction, biochemical characterization, and health effects of native and degraded fucoidans from *Sargassum crispifolium*. *Polymers*, 14 (2022) 1812.
16 Shao P, Pei YP, Fang ZX & Sun PL, Effects of partial desulfation on antioxidant and inhibition of DLD cancer cell of *Ulva fasciata* polysaccharide. *Int J Biol Macromol*, 65 (2014) 307.
17 Yang WN, Chen PW & Huang CY, Compositional characteristics and *in vitro* evaluations of antioxidant and neuroprotective properties of crude extracts of fucoidan prepared from compressional puffing-pretreated *Sargassum crassifolium*. *Mar Drugs*, 15 (2017) 183.
18 Huang CY, Kuo CH & Chen PW. Compressional-puffing pretreatment enhances neuroprotective effects of fucoidans from the brown seaweed *Sargassum hemiphyllum* on 6-hydroxydopamine-induced apoptosis in SH-SY5Y cells, *Molecules*, 23 (2017) 78.
19 Qi H, Tang S, Bian B, Lai C, Chen Y, Ling Z & Yong Q, Effect of H_2O_2-VC degradation on structural characteristics and immunomodulatory activity of larch arabinogalactan. *Front Bioeng Biotechnol*, 12 (2024) 1461343.
20 Ofoedu CE, You L, Osuji CM, Iwouno JO, Kabuo NO, Ojukwu M, Agunwah IM, Chacha JS, Muobike OP & Agunbiade AO, Hydrogen peroxide effects on natural-sourced polysacchrides: Free radical formation/production, degradation process, and reaction mechanism-a critical synopsis. *Foods*, 10 (2021) 699.
21 Jeong S, Lee S, Lee G, Hyun J & Ryu B, Systematic characteristics of fucoidan: Intriguing features for new pharmacological interventions. *Int J Mol Sci*, 25 (2024) 11771.
22 Chen CY, Wang SH, Huang CY, Dong CD, Huang CY, Chang CC & Chang JS, Effect of molecular mass and sulfate content of fucoidan from *Sargassum siliquosum* on antioxidant, anti-lipogenesis, and anti-inflammatory activity. *J Biosci Bioeng*, 132 (2021) 359.
23 Iwata A, Yamamoto-Fujimura M, Fujiwara S, Tajima S, Shigeyama T, Tsukimoto M, Ibuki T & Kataoka-Kato A, Incorporation of silver into sulfate groups enhances antimicrobial and antiviral effects of fucoidan. *Mar Drugs*, 22 (2024) 486.
24 Wu TC, Hong YH, Tsai YH, Hsieh SL, Huang RH, Kuo CH & Huang CY, Degradation of *Sargassum crassifolium* fucoidan by ascorbic acid and hydrogen peroxide, and compositional, structural, and *in vitro* anti-lung cancer analyses of the degradation products. *Mar Drugs*, 18 (2020) 334.

25 Pérez-Cruz C, Moraleda-Montoya A, Liébana R, Terrones O, Arrizabalaga U, García-Alija M, Lorizate M, Martínez Gascueña A, García-Álvarez I & Nieto-Garai JA, Mechanisms of recalcitrant fucoidan breakdown in marine *Planctomycetota*. *Nat Commun*, 15 (2024) 10906.

26 Uyen NTT, Yang AWH, Nguyen Q-AN, Hung A, Ngo ST & Lenon GB, Fucoidan for lung cancer therapy: A review of classification, mechanisms, and preclinical studies. *ACS Omega*, 10 (2025) 58012.

27 Yue Q, Liu Y, Li F, Hong T, Guo S, Cai M, Zhao L, Su L, Zhang S & Zhao C, Antioxidant and anticancer properties of fucoidan isolated from *Saccharina Japonica* brown algae. *Sci Rep*, 15 (2025) 8962.

28 He Z, Zhu B, Deng L & You L, Effects of UV/H_2O_2 degradation on the physicochemical and antibacterial properties of fucoidan. *Mar Drugs*, 22 (2024) 209.

29 Yao W, Yong J, Lv B, Guo S, You L, Cheung PCK & Kulikouskaya VI, Enhanced *in vitro* anti-photoaging effect of degraded seaweed polysaccharides by UV/H_2O_2 treatment. *Mar Drugs*, 21 (2023) 430.

30 Ponce NMA & Stortz CA, A comprehensive and comparative analysis of the fucoidan compositional data across the *Phaeophyceae*. *Front Plant Sci*, 11 (2020) 556312.

31 Palanisamy S, Vinosha M, Marudhupandi T, Rajasekar P & Prabhu NM, Isolation of fucoidan from *Sargassum polycystum* brown algae: Structural characterization, *in vitro* antioxidant and anticancer activity. *Int J Biol Macromol*, 102 (2017) 405.

32 Tako M, Nakada T & Hongou F, Chemical characterization of fucoidan from commercially cultured *Nemacystus decipiens* (Itomozuku). *Biosci Biotechnol Biochem*, 63 (1999) 1813.

33 Immanuel G, Sivagnanavelmurugan M, Marudhupandi T, Radhakrishnan S & Palavesam A, The effect of fucoidan from brown seaweed *Sargassum wightii* on WSSV resistance and immune activity in shrimp *Penaeus monodon* (Fab). *Fish Shellfish Immunol*, 32 (2012) 551.

34 Ermakova S, Sokolova R, Kim SM, Um BH, Isakov V & Zvyagintseva T, Fucoidans from brown seaweeds *Sargassum hornery*, *Eclonia cava*, *Costaria costata*: Structural characteristics and anticancer activity. *Appl Biochem Biotechnol*, 164 (2011) 841.

35 Kumar TV, Lakshmanasenthil S, Geetharamani D, Marudhupandi T, Suja G & Suganya P, Fucoidan - A α-d-glucosidase inhibitor from *Sargassum wightii* with relevance to type 2 diabetes mellitus therapy. *Int J Biol Macromol*, 72 (2015) 1044.

36 Bilan MI, Grachev AA, Shashkov AS, Nifantiev NE & Usov AI, Structure of a fucoidan from the brown seaweed *Fucus serratus* L. *Carbohydr Res*, 341 (2006) 238.

37 Dore CMPG, Alves MGdCF, Will LSEP, Costa TG, Sabry DA, de Souza Rêgo LAR, Accardo CM, Rocha HAO, Filgueira LGA & Leite EL, A sulfated polysaccharide, fucans, isolated from brown algae *Sargassum vulgare* with anticoagulant, antithrombotic, antioxidant and anti-inflammatory effects. *Carbohydr Polym*, 91 (2013) 467.

38 Vishchuk OS, Ermakova SP & Zvyagintseva TN, Sulfated polysaccharides from brown seaweeds *Saccharina japonica* and *Undaria pinnatifida*: Isolation, structural characteristics, and antitumor activity. *Carbohydr Res*, 346 (2011) 2769.

39 Ummat V, Sivagnanam SP, Rai DK, O'Donnell C, Conway GE, Heffernan SM, Fitzpatrick S, Lyons H, Curtin J & Tiwari BK, Conventional extraction of fucoidan from Irish brown seaweed *Fucus vesiculosus* followed by ultrasound-assisted depolymerization. *Sci Rep*, 14 (2024) 6214.

40 Li Y, McGowan E, Chen S, Santos J, Yin H & Lin Y, Immunopotentiating activity of fucoidans and relevance to cancer immunotherapy. *Mar Drugs*, 21 (2023) 128.

41 Koyanagi S, Tanigawa N, Nakagawa H, Soeda S & Shimeno H, Oversulfation of fucoidan enhances its anti-angiogenic and antitumor activities. *Biochem Pharmacol*, 65 (2003) 173.

42 Tripathi D, Ramar M, Lavudi K, Sharma S, Rajinikanth P & Pandey P, The potential of fucoidans from ocean treasures to biomedical marvels: A review. *Int J Biol Macromol*, 333 (2025) 148979.

43 Liu Y, Gao L & Yu Z, Revealing the complexity of polysaccharides: Advances in nmr spectroscopy for structural elucidation and functional characterization. *Appl Sci*, 15 (2025) 5246.

44 Peng Z, Gillissen B, Richter A, Sinnberg T, Schlaak MS & Eberle J, Enhanced apoptosis and loss of cell viability in melanoma cells by combined inhibition of ERK and Mcl-1 is related to loss of mitochondrial membrane potential, caspase activation and upregulation of proapoptotic Bcl-2 proteins. *Int J Mol Sci*, 24 (2023) 4961.

45 Lu CY, Qiu WL, Chao CH, Lu MK & Chang CC, A highly sulfated α-1, 4-linked galactoglucan of *Antrodia cinnamomea* with anti-inflammatory and anti-cancer activities. *Carbohydr Polym*, 364 (2025) 123810.

46 Zhang Y, Nie R, Liu W, Dong S, Yang J, Wang X, Wang Y & Zheng L, Sulfation on polysaccharides from *Zizania latifolia* extracted using ultrasound: Characterization, antioxidant and anti-non-small cell lung cancer activities. *Ultrason Sonochem*, 103 (2024) 106803.

47 Mustafa M, Ahmad R, Tantry IQ, Ahmad W, Siddiqui S, Alam M, Abbas K, Moinuddin, Hassan MI & Habib S, Apoptosis: A comprehensive overview of signaling pathways, morphological changes, and physiological significance and therapeutic implications. *Cells*, 13 (2024) 1838.

48 Lee YS, Kalimuthu K, Park YS, Luo X, Choudry MHA, Bartlett DL & Lee YJ, BAX-dependent mitochondrial pathway mediates the crosstalk between ferroptosis and apoptosis. *Apoptosis*, 25 (2020) 625.

49 Morse PT, Arroum T, Wan J, Pham L, Vaishnav A, Bell J, Pavelich L, Malek MH, Sanderson TH & Edwards BF, Phosphorylations and acetylations of cytochrome c control mitochondrial respiration, mitochondrial membrane potential, energy, ROS, and apoptosis. *Cells*, 13 (2024) 493.

50 Paul JP, Anticancer potential of fucoidan extracted from *Padina distromatica* Hauck (brown seaweed) from Hare Island, Thoothukudi, Tamil Nadu, India. *Asian J Pharm Sci Technol*, 4 (2014) 217.

51 Marudhupandi T, Kumar TTA, Lakshmanasenthil S, Suja G & Vinothkumar T, *In vitro* anticancer activity of fucoidan from *Turbinaria conoides* against A549 cell lines. *Int J Biol Macromol* 72 (2015) 919.

52 Hong OY, Jang HY, Lee YR, Jung SH, Youn HJ & Kim JS, Inhibition of cell invasion and migration by targeting matrix metalloproteinase-9 expression via sirtuin 6 silencing in human breast cancer cells. *Sci Rep*, 12 (2022) 12125.

53 Yin L, Sun C, Zhang J, Li Y, Wang Y, Bai L & Lei Z, Critical signaling pathways in osteoclast differentiation and bone resorption: Mechanisms and therapeutic implications

for periprosthetic osteolysis. *Front Cell Dev Biol* 13 (2025) 1639430.

54 Acuff HB, Carter KJ, Fingleton B, Gorden DL & Matrisian LM, Matrix metalloproteinase-9 from bone marrow-derived cells contributes to survival but not growth of tumor cells in the lung microenvironment. *Cancer Res*, 66 (2006) 259.

55 Huang TH, Chiu YH, Chan YL, Chiu YH, Wang H, Huang KC, Li TL, Hsu KH & Wu CJ, Prophylactic administration of fucoidan represses cancer metastasis by inhibiting vascular endothelial growth factor (VEGF) and matrix metalloproteinases (MMPs) in Lewis tumor-bearing mice. *Mar Drugs*, 13 (2015) 1882.

56 Wu Z, Huang Y, Hu W, Ren L, Jiang P, Margolskee RF, Wang H & Feng S, Lipopolysaccharide-induced inflammation increases nitric oxide production in taste buds. *Brain Behav Immun*, 103 (2022) 145.

57 Apostolova E, Lukova P, Baldzhieva A, Katsarov P, Nikolova M, Iliev I, Peychev L, Trica B, Oancea F & Delattre C, Immunomodulatory and anti-inflammatory effects of fucoidan: A review. *Polymers*, 12 (2020) 2338.

58 Tabarsa M, Dabaghian EH, You SG, Yelithao K, Cao RA, Rezaei M, Alboofetileh M & Bita S, The activation of NF-κB and MAPKs signaling pathways of RAW264. 7 murine macrophages and natural killer cells by fucoidan from *Nizamuddinia zanardinii*. *Int J Biol Macromol*, 148 (2020) 56.

59 Jiang Z, Okimura T, Yamaguchi K & Oda T, The potent activity of sulfated polysaccharide, ascophyllan, isolated from *Ascophyllum nodosum* to induce nitric oxide and cytokine production from mouse macrophage RAW264. 7 cells: Comparison between ascophyllan and fucoidan. *Nitric Oxide*, 25 (2011) 407.

60 Zayed A & Ulber R, Fucoidans: Downstream processes and recent applications. *Mar Drugs*, 18 (2020) 170.

61 Ting YS, Freeman KC, Kobayashi C, De Silva GM & Bland-Hawthorn J, Principal component analysis on chemical abundances spaces. *Mon Not R Astron Soc*, 421 (2012) 1231.

62 Ma M, Mu T & Zhou L, Identification of saprophytic microorganisms and analysis of changes in sensory, physicochemical, and nutritional characteristics of potato and wheat steamed bread during different storage periods. *Food Chem*, 348 (2021) 128927.